LETTER TO THE EDITOR

Journal of Non-Crystalline Solids 357 (2011) 1232–1234

Contents lists available at ScienceDirect

Journal of Non-Crystalline Solids

journal homepage: www.elsevier.com/ locate/ jnoncrysol

Letter to the Editor

Bulk metallic glasses based on ytterbium and calcium

J.Q. Wang [a], J.Y. Qin [b], X.N. Gu [c], Y.F. Zheng [c], H.Y. Bai [a,*]

[a] Institute of Physics, Chinese Academy of Sciences, Beijing 100190, PR China
[b] Department of Physics, University of Science and Technology of China, Hefei 230026, PR China
[c] Department of Advanced Materials and Nanotechnology, College of Engineering, Peking University, Beijing 100871, PR China

ARTICLE INFO

Article history:
Received 8 July 2010
Received in revised form 25 October 2010
Available online 14 December 2010

Keywords:
Metallic glass

ABSTRACT

We report the formation of a family of bulk metallic glasses (BMGs) based on rare earth element of ytterbium and alkaline earth element of calcium. The glass-forming ability, atomic packing density and corrosion behaviors of the BMGs show an extremum around the eutectic point with the change of the concentration of Yb and Ca.

Bulk metallic glasses (BMGs) have caught attention and interests because of their excellent properties such as high strength near the theoretical prediction, large elastic strain, and good corrosion and wear resistances [1–3]. The promising applications as mechanical structural materials, magnetic materials, bio-materials, and thermo-processable materials compel people to search new BMGs with good glass-forming ability (GFA) and novel properties [1–8]. It is recently found that the replacement of similar elements can obviously change the GFA and other properties [1,9,10]. Singularity phenomena and non-linear behaviors along with the change of compositions exist in various systems [9–14]. Among these singularities, the local symmetry [12], the atomic packing density [13], and liquid dynamic properties [14] have close relation with the mysterious glass-forming phenomenon. In this letter, we report the fabrication of a family of new bulk metallic glasses based on Yb and Ca. The glass-forming ability, reduced glass transition temperature (T_{rg}), thermal properties, mass density, and the corrosion properties are measured. It is found that these properties show non-linear relation with compositions and have an extremum around the eutectic point with the replacement of Yb by Ca.

The series of $Yb_{62.5-x}Ca_xZn_{20}Mg_{17.5}$ ($x=2.5$, 10, 20, 30, 40, 50, and 60) BMGs were cast into copper mold after induction melting of the base elements (purity better than 99.9 at.%) in a quartz tube under argon atmosphere. The amorphous states of the YbCa-based BMGs are testified by X-ray diffraction (XRD) in a MAC M03 XHF diffractometer (Cu K_α radiation) and by a differential scanning calorimeter (DSC, Perkin-Elmer DSC-7) under purified argon at 10 K/min heating rate (details can be found in Ref. [15]). The mass density was determined by the Archimedean technique in ethanol liquid. The mass was measured using an analytical balance with an accuracy of 0.01 mg. The repeated measuring error (in both air and ethanol) was better than ± 0.02 mg. Rod samples with the same size (2 mm in diameter) are adopted for the density measurement in order to rule out the cooling rate effect. The samples were prepared with weight bigger than 100 mg. So, the measuring error was better than 0.02%, and we can then track the changes of mass density with smaller experimental error. The polarization corrosion test was conducted in a 0.05 M Na_2SO_4 electrolyte. A three-electrode cell was used for electrochemical polarization tests (details can be found in Ref. [16]). The counter electrode was made of platinum and the reference electrode was saturated calomel electrode (SCE). All potentials quoted were on the SCE scale. The samples for corrosion test were closely sealed with epoxy resin and only leave an end-surface (with a cross-section area of about 3 mm^2) exposed to the solution. Prior to the test, the testing surface of each sample was mechanically polished to 1000#, and then degreased in acetone, distilled water and dried in air. The potential dynamic polarization curves of the samples were recorded at a scan rate of 1 mV/s when the open-circuit potential became almost steady.

Fig. 1(a) shows the XRD patterns of the $Yb_{62.5-x}Ca_xZn_{20}Mg_{17.5}$ ($x=2.5$, 10, 20, 31.25, 40, 50, and 60) BMGs in diameter of 2 mm. The curves show a broad maximum characteristic without obvious crystalline sharp peaks, denoting good GFA of the systems. The DSC traces with obvious glass transition and crystallization behaviors at a heating rate of 10 K/min are shown in Fig. 1(b)–(c). The characteristic temperatures in details are listed in Table 1. The glass transition temperatures (T_g) decrease monotonously along with the increasing of Ca concentration and has a sharp drop around $x=40$. The value of T_g ranges from 345 K to 376 K, and all of them are near or lower than the boiling temperature of water (373 K). The crystallized temperatures (T_x) range from 399 K to 380 K. These data indicate that the YbCa-based BMGs are another metallic plastic system [17] and would be a good candidate in thermal-plastic applications. Fig. 1(c) shows the melting part of the DSC traces. The melting temperatures T_m decrease monotonously from 650 K to 607 K. The liquid temperatures

* Corresponding author.
E-mail address: hybai@aphy.iphy.ac.cn (H.Y. Bai).

0022-3093/$ – see front matter © 2010 Elsevier B.V. All rights reserved.
doi:10.1016/j.jnoncrysol.2010.11.046

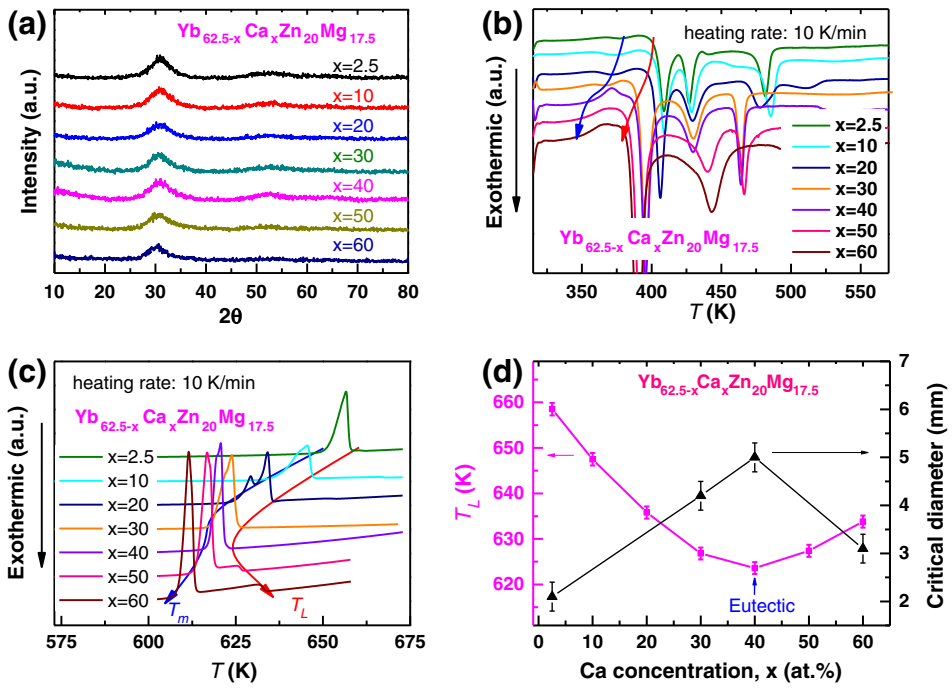

Fig. 1. (a) The XRD patterns of $Yb_{62.5-x}Ca_xZn_{20}Mg_{17.5}$ ($x=2.5$, 10, 20, 30, 40, 50, 60) BMGs with diameter of 2 mm. No obvious crystal peaks are found. (b) The DSC traces for the system show obvious glass transition behavior with low glass transition temperatures and wide supercooled range. (c) The melting part of the DSC traces. (d) The liquidus temperature T_L (magenta square symbols to the left axis) gets to minimum which indicates eutectic composition; the corresponding critical diameter for the totally amorphous rods (black triangles to the right axis).

T_l along with the concentration of Ca are shown in Fig. 1(d). It decreases from 659 K to 624 K till $x=40$ and increase to 634 K for $x=60$, which indicates that the eutectic point of the $Yb_{62.5-x}Ca_xZn_{20}Mg_{17.5}$ alloy system is close to $x=40$. According to the thermodynamic criterion of Cohen and Turnbull [18,19], the best GFA should be around the composition of $x=40$. We studied the critical glass-forming size [see Fig. 1(d)] and the critical diameter for rod samples is determined to be 2.0 mm, 4.2 mm, 5.0 mm and 3.0 mm for $x=2.5$, 30, 40, and 60, respectively. The best glass-forming composition corresponds to the eutectic position and fits the criterion of Cohen and Turnbull [18,19]. The fragility concept provides a measurement of the sensitivity of the structure of a liquid to temperature changes. The fragility can be quantified by the fragility parameter m as $\frac{m=d\log\tau}{dT_g/T|_{T=T_g}}$ [20]. By applying different heating rates, the thermodynamic m of the BMGs is determined [21,22]. The values of m for $Yb_{62.5-x}Ca_xZn_{20}Mg_{17.5}$ $x=2.5$, 30 and 60 are 24 ± 4, 28 ± 4, and 23 ± 4, respectively. This indicates a "strong" characteristic of the glass-forming liquid [20].

In CuZr systems, the compositions with high GFA tend to have bigger packing density [13], we then measured the mass density carefully and the data are shown in Fig. 2(a). The straight line with a slope of -0.0715 is drawn to guide the eyes. It is found that the experimental data deviate from the linear. In order to show the deviations, we scaled measured density plus the linear relation by $0.0715x$ (i.e., $\rho+0.0715x$) as shown in Fig. 2(b). One can see clearly that the density data reach a minimum around the eutectic point

Table 1
The values of T_g, T_x, T_m, T_l and $T_{rg}=T_g/T_l$ of typical $Yb_{62.5-x}Ca_xZn_{20}Mg_{17.5}$ BMGs.

$Yb_{62.5-x}Ca_xZn_{20}Mg_{17.5}$	T_g (K)	T_x (K)	T_m (K)	T_l (K)	T_{rg}
x=2.5	376	399	650	659	0.571
x=10	373	399	635	647	0.576
x=20	371	396	625	636	0.584
x=30	367	385	617	627	0.586
x=40	355	387	616	624	0.569
x=50	347	381	613	627	0.554
x=60	345	380	607	634	0.544

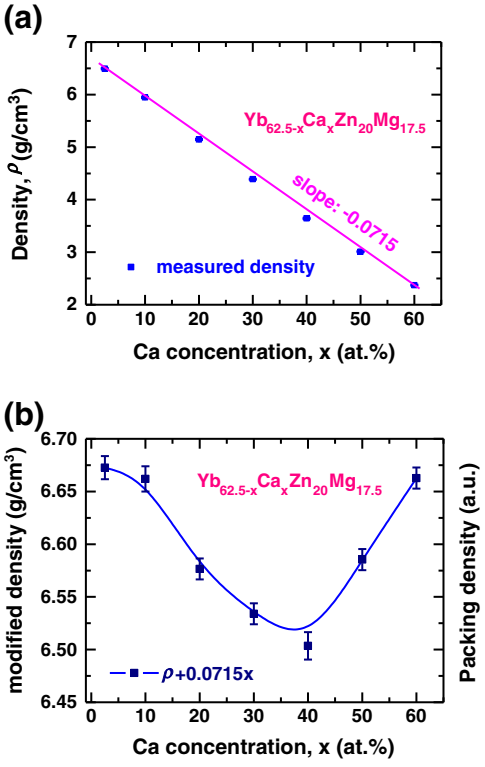

Fig. 2. (a) The filled dots represent the measured density along with changing the concentration of Ca. The line with slope of -0.0715 is drawn to guide the eyes. (b) The measured density modified by plus $0.0715x$. It can be seen clearly that the density doesn't decrease linearly with the increase of Ca, but has a minimum around eutectic point.

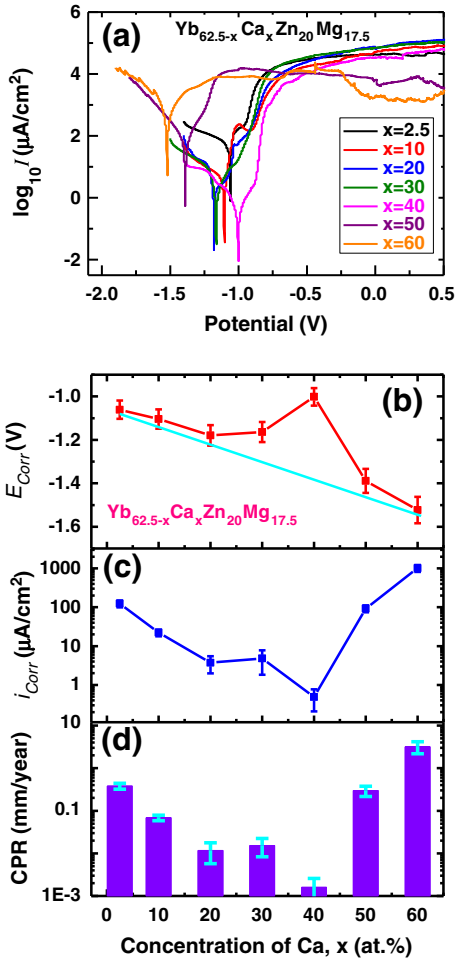

Fig. 3. (a) The potentiodynamic polarization curves of the $Yb_{62.5-x}Ca_xZn_{20}Mg_{17.5}$ ($x=2.5$, 10, 20, 30, 40, 50, 60) BMGs. (b) the corrosion potential (E_{corr}), (c) the corrosion current density (i_{corr}), and (d) the corrosion penetration rate (CPR) at E_{corr} for the Yb and Ca co-based BMGs. The corrosion behavior shows highest corrosion resistance around $x=40$ corresponding to the change tendency of GFA and density.

$x=40$, which indicates that the higher atomic packing density does not induce high GFA for YbCa-based BMGs.

We also studied the potentiodynamic polarization corrosion behaviors for the $Yb_{62.5-x}Ca_xZn_{20}Mg_{17.5}$ ($x=2.5$ to 60) BMGs in a 0.05 M Na_2SO_4 electrolyte, as shown in Fig. 3(a). The corrosion potential (E_{corr}) versus the concentration of Ca is shown in Fig. 3(b), and the E_{corr} exhibits singularity around $x=40$. Corrosion potential represents the ability of losing electrons for a material. The lower E_{corr} means the alloy is easier to lose the electrons. The mixing of Yb and Ca tends to increase the corrosion potential comparing to the linear relation [as shown in Fig. 3(b)]. The corrosion current density (i_{corr}) calculated according to the Stern–Geary method (or polarization–resistance method) [23], also gets to the lowest for the $x=40$ sample. The corrosion penetration rate (CPR) at E_{corr} depends on the inherent material and electrolyte properties and can be determined from the corrosion current density (i_{corr}) by the application of Faraday's law [24,25]. The CPR is used to evaluate the corrosion rate at E_{corr}. According to Faraday's law, it can be expressed as, $CPR(\mu m/year)=0.327Mi_{corr}/m\rho$, where M is the atomic weight (g/mol), m is the average oxidation valence, and ρ is the mass density (g/cm^3). As shown in Fig. 3(d), the corrosion rate of the YbCa-based BMG can be enhanced by more than 1000 times than that of Yb- or Ca-based BMGs. The eutectic composition with the lowest packing density has the best corrosion resistance. The continuously tunable corrosion properties may allow the BMGs to be applied as bio-materials [4,5].

In summary, the YbCa-based BMGs have excellent glass-forming ability, high corrosion resistance, and the lowest packing density around the eutectic point. The combination of low glass transition temperature and tunable corrosion resistance makes the system a good candidate for applications in thermal plasticity and bio-materials.

Acknowledgements

Financial support is from the NSF of China (nos. 50731008 and 50921091) and MOST 973 of China (nos. 2007CB613904 and 2010CB731603).

References

[1] A. Inoue, Acta Mater. 48 (2000) 279.
[2] (a) W.H. Wang, C. Dong, C.H. Shek, Mater. Sci. Eng. R 44 (2004) 45;
(b) W.H. Wang, M.P. Macht, H. Wollenberger, Appl. Phys. Lett. 71 (1997) 58;
(c) B.C. Wei, Y. Zhang, Y.X. Zhuang, D.Q. Zhao, M.X. Pan, W.H. Wang, J. Appl. Phys. 89 (2001) 3529;
(d) B.C. Wei, W. Löser, L. Xia, S. Roth, M.X. Pan, W.H. Wang, J. Eckert, Acta Mater. 50 (2002) 4357.
[3] (a) W.H. Wang, Adv. Mater. 21 (2009) 4524;
(b) Q. Luo, W.H. Wang, J. Non Cryst. Solids 355 (2009) 759.
[4] B. Zberg, P.J. Uggowitzer, J.F. Löffler, Nat. Mater. 8 (2009) 887.
[5] J. Schroers, G. Kumar, T.M. Hodges, S. Chan, T.R. Kyriakides, JOM 61 (2009) 21.
[6] G. Kumar, H.X. Tang, J. Schroers, Nature 457 (2009) 868.
[7] A.L. Greer, Science 267 (1995) 1947.
[8] W.L. Johnson, MRS Bull. 24 (1999) 42.
[9] (a) J.Q. Wang, P. Yu, H.Y. Bai, J. Non Cryst. Solids 354 (2008) 5440;
(b) S. Li, R.J. Wang, M.X. Pan, D.Q. Zhao, W.H. Wang, J. Non Cryst. Solids 354 (2008) 1080.
[10] R. Li, S.J. Pang, C.L. Ma, T. Zhang, Acta Mater. 55 (2007) 3719.
[11] W.H. Wang, Prog. Mater. Sci. 52 (2007) 540.
[12] X.K. Xi, L.L. Li, B. Zhang, W.H. Wang, Y. Wu, Phys. Rev. Lett. 99 (2007) 095501.
[13] Y. Li, Q. Guo, J.A. Kalb, C.V. Thompson, Science 322 (2008) 1816.
[14] S.M. Chathoth, B. Damaschke, J.P. Embs, K. Samwer, Appl. Phys. Lett. 95 (2009) 191907.
[15] J.Q. Wang, W.H. Wang, H.Y. Bai, Appl. Phys. Lett. 94 (2009) 041910.
[16] X.N. Gu, Y.F. Zheng, S.P. Zhong, T.F. Xi, J.Q. Wang, W.H. Wang, Biomaterials 31 (2010) 1093.
[17] (a) B. Zhang, D.Q. Zhao, M.X. Pan, W.H. Wang, A.L. Greer, Phys. Rev. Lett. 94 (2005) 205502;
(b) J.F. Li, J.Q. Wang, X.F. Liu, K. Zhao, B. Zhang, H.Y. Bai, M.X. Pan, W.H. Wang, Sci. China G Phys. Mech. Astron. 53 (2010) 409.
[18] M.H. Cohen, D. Turnbull, Nature 189 (1961) 131.
[19] D. Turnbull, Contemp. Phys. 10 (1969) 473.
[20] C.A. Angell, Science 267 (1995) 1924.
[21] R. Brüning, K. Samwer, Phys. Rev. B 46 (1992) 11318.
[22] R. Böhmer, K.L. Ngai, C.A. Angell, D.J. Plazek, J. Chem. Phys. 99 (1993) 4201.
[23] M. Stern, A.L. Geary, J. Electrochem. Soc. 104 (1957) 56.
[24] M.L. Morrison, R.A. Buchanan, O.N. Senkov, D.B. Miracle, P.K. Liaw, Metal. Mater. Trans. A 37A (2006) 1239.
[25] E.E. Stansbury, R.A. Buchanan, Fundamentals of Electrochemical Corrosion, ASM International, Materials Park, OH, 2000.